

Resonant two-photon ionization spectroscopy of LiCu

Larry M. Russon, Gretchen K. Rothschof, and Michael D. Morse
Department of Chemistry, University of Utah, Salt Lake City, Utah 84112

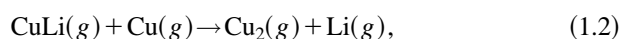
(Received 22 May 1996; accepted 8 April 1997)

Jet-cooled LiCu has been investigated using resonant two-photon ionization spectroscopy. A long vibrational progression was observed and identified as the $[20.5] \ ^1\Sigma^+ \leftarrow X \ ^1\Sigma^+$ band system. Ten bands of the system were rotationally resolved for $^7\text{Li}^{63}\text{Cu}$, giving bond lengths of $r_0 = 2.2618(3) \text{ \AA}$ for the $X \ ^1\Sigma^+$ state and $r'_e = 2.74(4) \text{ \AA}$ for the $[20.5] \ ^1\Sigma^+$ state. The fitted spectroscopic parameters of the $[20.5] \ ^1\Sigma^+$ state were used to obtain a RKR estimate of the $[20.5] \ ^1\Sigma^+$ potential energy curve. The unusual shape of this curve is thought to derive from avoided crossings between the Li^+Cu^- ion pair state and covalent states, with the Li^+Cu^- ion pair state ultimately correlating to the ground electronic state of the molecule. © 1997 American Institute of Physics. [S0021-9606(97)01427-X]

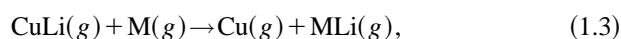
I. INTRODUCTION

For the past several years work in this laboratory has concentrated on the spectroscopy of diatomic transition metal molecules, with particular attention devoted to the $3d$ series.¹ From this work we have gained a significant understanding of the bonding interactions between atoms with open d subshells. More recently, the chemical bonding between transition metals and aluminum, a main group metal, has been investigated to probe the chemical bonding between the p -block and d -block metals and to understand the role of the d orbitals in such interactions.² Here we further extend these studies of the interaction between main group metals and transition metals by investigating the spectroscopy of diatomic LiCu, which provides a model for the interaction between alkali metals and transition metals having stable $3d^{n+1}4s^1$ configurations. In a subsequent paper we will present results on the spectroscopy of LiCa, which provides a model for the interaction between alkali metal and transition metals having stable $3d^n4s^2$ configurations.³ It is our hope that systematic investigations of the chemical bonding between transition metals and lithium will aid in understanding the enhanced catalytic activity of transition metal surfaces on which alkali metals have been preadsorbed. The alkali metals serve as promoters, donating their valence electron to the transition metal substrate. This has been shown to dramatically reduce the work function of the catalyst and substantially increase the rate of dissociative chemisorption of molecules such as CO, N₂, and NO.⁴

Apart from the work on LiCu and LiAg published earlier this year by Brock *et al.*, which provides vibrationally resolved spectra of 12 band systems of LiCu lying within the range 29 500–36 200 cm⁻¹,⁵ the only previous experimental work on LiCu of which we are aware is a Knudsen effusion mass spectrometric determination of the dissociation energy by Neubert and Zmbov in 1974.⁶ They report $D_0(\text{LiCu}) = 1.96 \pm 0.09 \text{ eV}$ based on an analysis of the reactions,



and



where M is Ag or Au.

A more precise value of the ground state bond energy ($D_0 = 1.9451 \pm 0.0015 \text{ eV}$) is derived in the paper by Brock *et al.*, who assume that the observed F state vibrational progression converges to the $\text{Li } 1s^2 2p^1, \ ^2P^0 + \text{Cu}, \ 3d^{10} 4s^1, \ ^2S$ separated atom limit, which lies 14 904 cm⁻¹ above ground state atoms.⁵ Either of the other two possible separated atom limits of $\text{Li } 1s^2 2s^1, \ ^2S + \text{Cu}, \ 3d^9 4s^2, \ ^2D_{5/2}$ (at 11 203 cm⁻¹) (Ref. 7) or $\text{Li } 1s^2 2s^1, \ ^2S + \text{Cu}, \ 3d^9 4s^2, \ ^2D_{3/2}$ (at 13 245 cm⁻¹) (Ref. 7) lead to estimated bond energies (2.404 and 2.151 eV, respectively) lying considerably outside of the error limits proposed by Neubert and Zmbov.⁶ This lends credence to the assignment of the convergence limit of the F state proposed by Brock *et al.*, and considerably improves the precision of the bond energy of LiCu.

On the theoretical side, Beckmann and co-workers⁸ carried out pseudopotential configuration interaction calculations on LiCu in 1985 and then tested the interaction of the molecule with atomic hydrogen. They report a ground state bond energy of 1.30 eV and a bond length of 2.6 Å for LiCu, with a somewhat polar bond in which lithium carries a +0.20 partial charge. More recently (1987) Bauschlicher *et al.* performed more extensive ab initio calculations on LiCu (Ref. 9) giving $D_e = 1.75 \text{ eV}$, $r_e = 2.296 \text{ \AA}$, and $\omega_e = 379 \text{ cm}^{-1}$ with a partial charge on lithium of +0.24 and a dipole moment of 4.636 D. They report that the bonding in the molecule is quite ionic. Most recently, Lawson and Harrison have reported ab initio calculations on several LiM and LiM⁺ molecules (M=Sc, Ti, V, Cr, and Cu) using a multi-configurational self-consistent field (MCSCF) method including four f functions (contracted to 3) on the copper atom.¹⁰ For neutral LiCu the calculation resulted in $D_e = 1.616 \text{ eV}$, $r_e = 2.428 \text{ \AA}$, and $\omega_e = 356 \text{ cm}^{-1}$ for the $^1\Sigma^+$ ground state. For the LiCu⁺ cation, a considerably weaker bond was found with $D_e = 0.71 \text{ eV}$, $r_e = 2.913 \text{ \AA}$, and $\omega_e = 220 \text{ cm}^{-1}$ for the $^2\Sigma^+$ ground state.¹⁰

In this paper an investigation of the electronic spectroscopy of LiCu is reported, employing the technique of resonant two-photon ionization spectroscopy. In Sec. II the ex-

perimental apparatus is briefly described and Sec. III presents experimental results. In Sec. IV the electronic nature of the $X^1\Sigma^+$ and $[20.5]^1\Sigma^+$ states is discussed. Section V then concludes the paper with a summary of the most important findings.

II. EXPERIMENT

The instrument used in this study has been previously employed for transition metal cluster cation photodissociation experiments.¹¹ For the present experiments a modified ion acceleration source was used, and the timings of the ion extraction pulses were adjusted to allow for photoionization experiments. The metal sample consisted of a disk which was formed by melting a 3:2 Li:Cu molar mixture in an electric arc furnace under an argon atmosphere. The resulting alloy was machined flat on one side and mounted in a mechanism that rotates and translates the sample against a stainless steel vaporization block.¹² The output radiation from a KrF excimer laser (248 nm, 10–15 mJ/pulse) was focused onto the sample disk and timed to fire during a pulse of helium carrier gas (approximately 120 psig backing pressure), which swept over the metal target. This produced a metal plasma which was carried down a 3 cm long, 2 mm diam clustering region before expanding supersonically through a conical nozzle into a low pressure chamber (10^{-4} Torr). The metal cluster beam was then roughly collimated by a 6.5 mm skimmer as it entered a differentially pumped ionization region. The LiCu molecules were cooled to a rotational temperature of roughly 20 K, although a strong high- J tail to the rotational distribution was readily observed. No identifiable vibrational hot bands were observed, indicating a vibrational temperature below 250 K.

The metal cluster beam was interrogated by the output of an excimer-pumped dye laser and the resulting excited electronic states were ionized by a portion of the 308 nm (XeCl) excimer laser radiation which pumps the dye laser, or by frequency doubled dye laser radiation. Ions produced in this way were accelerated into a reflectron time-of-flight mass spectrometer by a Wiley–McLaren acceleration assembly.¹³ The mass separated ions were detected with a dual microchannel plate detector, and the resulting signal was preamplified, digitized, and averaged in a 386DX-based personal computer.

Rotationally resolved spectra were calibrated by comparing a simultaneously recorded I_2 absorption spectrum with that reported by Gerstenkorn and Luc.¹⁴ For all of the bands reported here the dye laser radiation fell outside of the range of the I_2 atlas. To obtain a useful calibration spectrum the dye laser radiation was Raman shifted by focusing it through a 500 psi H_2 gas cell. As described by Clouthier and Karolczak,¹⁵ the stimulated Raman scattering process occurs only on the $Q(1)$ line, giving a precise Raman shift of 4155.163 cm^{-1} for 500 psi H_2 , bringing the dye laser radiation back into the range of the I_2 atlas. For the experiments reported here, the dye laser radiation intersected the molecular beam at right angles, so no Doppler correction was required.

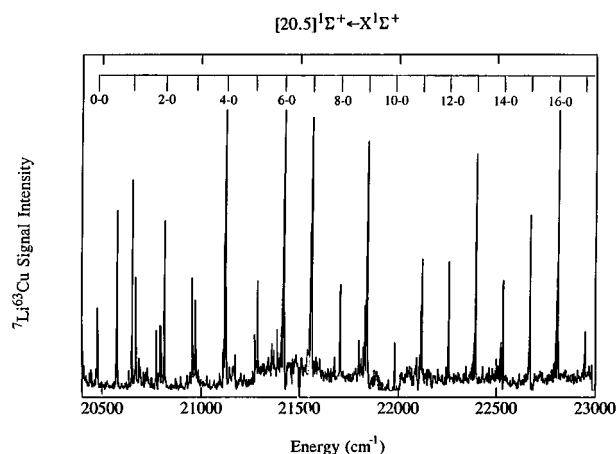


FIG. 1. A low resolution scan over a portion of the $[20.5]^1\Sigma^+ \leftarrow X^1\Sigma^+$ band system. This figure is a composite of three scans using the coumarin laser dyes C480, C460, and C440 for excitation and 308 nm radiation for photoionization. Because no correction was made for the variation in dye laser intensity across the band system, the relative band intensities are inaccurate in this figure.

III. RESULTS

A. The $[20.5]^1\Sigma^+ \leftarrow X^1\Sigma^+$ band system

Data were collected over a range of $16\,400\text{ cm}^{-1}$ to $24\,900\text{ cm}^{-1}$ using the fundamental dye laser radiation for excitation and the 308 nm XeCl radiation or frequency doubled dye laser radiation for ionization. Although many vibronic bands were observed throughout the regions above $20\,400\text{ cm}^{-1}$, the range from $20\,500\text{ cm}^{-1}$ to $24\,900\text{ cm}^{-1}$, was dominated by one strong progression. A portion of this band system is displayed in Fig. 1. Overall, 27 bands were observed in this progression corresponding to $v' = 0$ bands with v' in the range of 0–31. The vibronic band positions for this system are reported for $^7\text{Li}^{63}\text{Cu}$ and $^7\text{Li}^{65}\text{Cu}$ in Table I.

The vibrational numbering of the bands was established using the isotope shift, $\nu_0(^7\text{Li}^{63}\text{Cu}) - \nu_0(^7\text{Li}^{65}\text{Cu})$, as measured from fitted band origins for the 6-0, 7-0, 9-0, 10-0, 12-0, 14-0, and 16-0 bands. The measured isotope shifts are plotted in Fig. 2 as a function of band frequency, and for three different vibrational numberings of the system this is compared to the theoretically predicted isotope shift, given by¹⁶

$$\nu_i - \nu_j = (\omega'_i - \omega''_i)(1 - \rho_{ij})/2 + (\omega''_i x''_i - \omega'_i x'_i)(1 - \rho_{ij}^2)/4 + \omega'_i(1 - \rho_{ij})v' - \omega'_i x'_i(1 - \rho_{ij}^2)(v'^2 + v'). \quad (3.1)$$

Here $\rho_{ij} = (\mu_i/\mu_j)^{1/2}$, μ_i is the reduced mass of the i th isotopic combination, and the values of $\omega''_e(465.9\text{ cm}^{-1})$ and $\omega''_e x''_e(4.11\text{ cm}^{-1})$ were taken from the work of Brock *et al.*⁵ The curve giving the best agreement between measured and predicted isotope shifts corresponds to the assignment given in Fig. 1 and Table I. The poor agreement of the other two assignments, which change the numbering by ± 1 , establishes the validity of the assignment.

Although 10 bands of $^7\text{Li}^{63}\text{Cu}$ and 7 bands of $^7\text{Li}^{65}\text{Cu}$ were successfully rotationally resolved and analyzed, several

TABLE I. Vibronic band positions (in cm^{-1}) of the $[20.5] \ ^1\Sigma^+ \leftarrow X \ ^1\Sigma^+$ system of LiCu.

Band	$^7\text{Li}^{63}\text{Cu}$			$^7\text{Li}^{65}\text{Cu}$			Isotope shift ^a
	Observed frequency	Calculated frequency	Residual	Observed frequency	Calculated frequency	Residual	
0-0	20 477.7	20 548.97	-71.3 ^b	20 477.7	20 547.64	-69.9 ^b	0.0
1-0	20 648.9	20 698.84	-49.9 ^b	20 648.8	20 697.71	-48.9 ^b	0.1
2-0	20 813.6	20 846.51	-32.9 ^b	20 813.4	20 845.50	-32.1 ^b	0.2
3-0	20 968.7	20 992.27	-23.6 ^b	20 968.8	20 991.30	-22.5 ^b	-0.1
4-0	21 122.3	21 136.36	-14.1 ^b	21 121.3	21 135.38	-14.1 ^b	1.0
5-0	21 266.8	21 279.03	-12.2 ^b	21 265.7	21 277.98	-12.3 ^b	1.1
6-0	21 419.700 ^{c,d}	21 420.50	-0.80	21 418.584 ^{c,e}	21 419.35	-0.8	1.116 ^f
7-0	21 561.118 ^{c,d}	21 561.00	0.12	21 559.773 ^{c,e}	21 559.69	0.1	1.345 ^f
8-0	21 701.7	21 700.71	1.0 ^b	21 702.1	21 699.22	2.9 ^b	-0.4
9-0	21 841.108 ^{c,d}	21 839.80	1.31	21 839.367 ^{c,e}	21 838.12	1.2	1.741 ^f
10-0	21 979.149 ^{c,d}	21 978.45	0.70	21 977.209 ^{c,e}	21 976.54	0.7	1.940 ^f
11-0	22 117.1	22 116.80	0.3 ^b	22 114.9	22 114.66	0.2 ^b	2.2
12-0	22 254.803 ^{c,d}	22 254.98	-0.18	22 252.432 ^{c,e}	22 252.59	-0.2	2.371 ^f
13-0	22 392.745 ^{c,d}	22 393.10	-0.36	22 390.3	22 390.47	-0.2	2.4
14-0	22 530.582 ^{c,d}	22 531.26	-0.68	22 527.628 ^{c,e}	22 528.39	-0.8	2.954 ^f
15-0	22 665.4	22 669.54	-4.1 ^b	22 662.4	22 666.43	-4.0 ^b	3.0
16-0	22 807.519 ^{c,d}	22 808.02	-0.50	22 804.286 ^{c,e}	22 804.67	-0.4	3.233 ^f
17-0	22 945.700 ^{c,d}	22 946.73	-1.03	22 941.9	22 943.15	-1.3	3.8
21-0	23 504.477 ^{c,d}	23 504.43	0.05	23 500.2	23 500.01	0.2	4.3
22-0	23 646.4	23 644.54	1.9	23 641.4	23 639.93	1.5	5.0
23-0	23 785.2	23 784.85	0.4	23 780.8	23 780.05	0.8	4.4
25-0	24 066.4	24 065.80	0.6	24 061.2	24 060.65	0.5	5.2
28-0	24 485.2	24 486.69	-1.5	24 479.4	24 480.98	-1.6	5.8
29-0	24 625.4	24 626.35	-0.9	24 619.4	24 620.43	-1.0	6.0
30-0	24 765.1	24 765.44	-0.3	24 759.2	24 759.29	-0.1	5.9
31-0	24 905.1	24 903.78	1.3	24 898.6	24 897.38	1.2	6.5

^aDefined as $\nu_0(^7\text{Li}^{63}\text{Cu}) - \nu_0(^7\text{Li}^{65}\text{Cu})$.

^bNot included in vibronic fit reported in Table II due to obvious perturbations or uncertain identification of the vibronic band.

^c ν_0 , measured in high resolution and calibrated using the absorption spectrum of I_2 .

^dFitted values of B'_v , for $^7\text{Li}^{63}\text{Cu}$ (in cm^{-1}); $B'_6=0.293\ 20(29)$; $B'_7=0.284\ 86(19)$; $B'_8=0.276\ 18(9)$; $B'_{10}=0.272\ 49(13)$; $B'_{12}=0.266\ 83(11)$; $B'_{13}=0.265\ 24(24)$; $B'_{14}=0.261\ 71(22)$; $B'_{16}=0.259\ 85(35)$; $B'_{17}=0.258\ 65(25)$; $B'_{21}=0.250\ 87(11)$.

^eFitted values of B'_v , for $^7\text{Li}^{65}\text{Cu}$ (in cm^{-1}); $B'_6=0.291\ 86(29)$; $B'_7=0.284\ 00(25)$; $B'_8=0.274\ 94(14)$; $B'_{10}=0.271\ 31(12)$; $B'_{12}=0.265\ 21(15)$; $B'_{14}=0.260\ 51(24)$; $B'_{16}=0.258\ 71(59)$.

^fMeasured in high resolution as $\nu_0(^7\text{Li}^{63}\text{Cu}) - \nu_0(^7\text{Li}^{65}\text{Cu})$.

of the observed bands displayed severe perturbations in the rotationally resolved spectra, preventing a rotational analysis. Thus, for example, the 8-0, 11-0, and 15-0 bands could not be rotationally analyzed. Likewise, it proved difficult to unambiguously identify the 0-0 through 5-0 bands because of numerous other bands in this low frequency region (see Fig. 1). None of the various possible assignments of the 0-0 through 5-0 bands fit into the regular pattern of vibronic levels established by a fit of the 6-0 through 31-0 bands, suggesting that these vibronic levels are perturbed by the other states which are obviously present in this spectral region. The 0-0 through 5-0 bands which are listed in Table I are simply the most likely candidates for these bands. In addition, the 18-0, 19-0, 20-0, 26-0, and 27-0 bands fell into spectral regions which were not scanned, and the 24-0 band displayed perturbations in the upper state. It appears that the entire band system is affected by perturbations, some of which lead to predissociation.

The vibronic bands which appeared to be free of perturbations (identified in Table I) were fitted to extract the vibra-

tional constants of the upper state according to the standard expression¹⁶

$$\begin{aligned} \nu_{v',-0} = & T_0 + \omega'_e[(v'+1/2)^1 - 1/2] - \omega'_e x'_e[(v'+1/2)^2 - 1/4] \\ & + \omega'_e y'_e[(v'+1/2)^3 - 1/8] \\ & + \omega'_e z'_e[(v'+1/2)^4 - 1/16], \end{aligned} \quad (3.2)$$

resulting in the excited state spectroscopic constants $T_0 = 20\ 548.97(8.88)\ \text{cm}^{-1}$, $\omega'_e = 152.34(2.74)\ \text{cm}^{-1}$, $\omega'_e x'_e = 1.318(252)\ \text{cm}^{-1}$, $\omega'_e y'_e = 0.0511(95)\ \text{cm}^{-1}$, and $\omega'_e z'_e = -0.000\ 67(13)\ \text{cm}^{-1}$ for $^7\text{Li}^{63}\text{Cu}$. These constants are only capable of reproducing the vibrational levels with $v' \geq 6$, since $v' = 0-5$ were excluded from the fit. The 0-0 through 5-0 bands were poorly identified, not rotationally resolved, and possibly subject to perturbations, so it was felt that they should not be included in the fit. Here and throughout this paper 1σ error limits are given in parentheses, in units of the last reported digits.

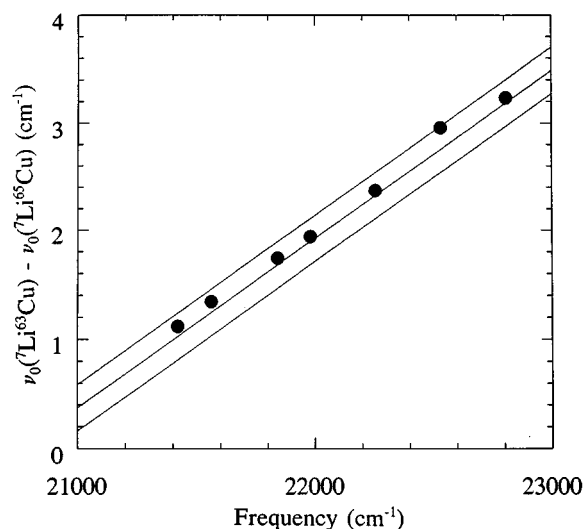


FIG. 2. Determination of the vibrational numbering of the band system, using isotope shift information. The isotope shift is plotted vs the band frequency for three sequential possible numberings of the vibrational bands and compared to the measured data points. The plot demonstrates that the 21 420 cm^{-1} band of $^7\text{Li}^{63}\text{Cu}$ is clearly the 6-0 band. Similar data using the isotope shifts between $^6\text{Li}^{63}\text{Cu}$ and $^7\text{Li}^{63}\text{Cu}$ also strongly support this assignment.

A rotationally resolved scan of the 9-0 band of $^7\text{Li}^{63}\text{Cu}$ is displayed in Fig. 3. This is typical of the appearance of the unperturbed bands. The spectrum displays *R* and *P* branches, but the *Q* branch is notably absent, indicating an $\Omega' = 0 \leftarrow \Omega'' = 0$ transition. Based on the expected $X^1\Sigma^+$ ground state, this identifies the upper state as a $^1\Sigma^+$ state as well. It will be designated as the $[20.5]^1\Sigma^+$ state, where the number in brackets designates the energy of the $v' = 0$ level, in thousands of wave numbers. The band is red shaded with a severe band head in the *R* branch, with the *R*(0) and *R*(1) lines coinciding within the resolution of the laser. This indicates a large increase in the bond length upon electronic

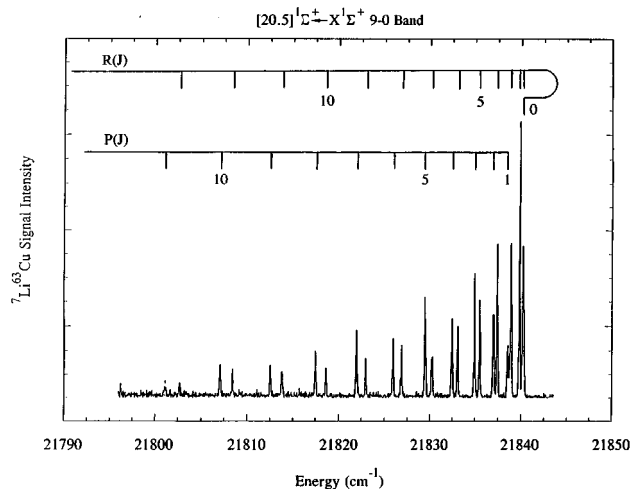


FIG. 3. The high resolution scan over the 9-0 band. The *R*(0) and *R*(1) lines are effectively coincident due to the large change in bond length upon electronic

excitation. As one progresses up the vibrational ladder the *P* and *R* branches become coincident and then separate again in higher vibrational bands. This phenomenon increased the uncertainty in the rotational line positions for several of the bands in which the branches were nearly coincident, leading to increased errors. Nevertheless, it was possible to fit ten of the $^7\text{Li}^{63}\text{Cu}$ vibronic bands to the usual expression,¹⁶

$$\nu = \nu_{v'-0} + B'_v J'(J'+1) - B''_0 J''(J''+1). \quad (3.3)$$

A simultaneous fit of all ten bands to Eq. (3.3) was used to provide a single value of B''_0 , giving $B''_0 = 0.522\,02(16)\,\text{cm}^{-1}$ for $^7\text{Li}^{63}\text{Cu}$, corresponding to $r''_0 = 2.2618(3)\,\text{\AA}$. Fitted values of the band origins are provided in Table I, along with fitted values of B'_v (see the footnotes to Table I). Seven of these ten bands were also fitted for the $^7\text{Li}^{65}\text{Cu}$ isotopic variant, providing $B''_0 = 0.519\,73(21)\,\text{cm}^{-1}$, corresponding to $r''_0 = 2.2633(5)\,\text{\AA}$. The fitted band origins for these seven bands were used for the isotopic determination of the absolute vibrational numbering as described above. Observed and fitted line positions for all of the rotationally resolved bands of $^7\text{Li}^{63}\text{Cu}$ and $^7\text{Li}^{65}\text{Cu}$ are available through the Physics Auxiliary Publication Service (PAPS) of the American Institute of Physics¹⁷ or from the author (M.D.M.).

In addition to fits of the individual bands, the values of B'_v for $^7\text{Li}^{63}\text{Cu}$ and $^7\text{Li}^{65}\text{Cu}$ were fitted to the expression¹⁶

$$B'_v = B'_e - \alpha'_e(v+1/2) + \gamma'_e(v+1/2)^2 + \delta'_e(v+1/2)^3, \quad (3.4)$$

leading to the rotation-vibration constants listed in Table II. The long extrapolation from B'_0 to B'_e introduces significant error in B'_e , which is evident in the large difference in r'_e values derived for $^7\text{Li}^{63}\text{Cu}$ and $^7\text{Li}^{65}\text{Cu}$. Because of this problem we recommend a value of $2.74 \pm 0.04\,\text{\AA}$ for r'_e .

B. The ionization energy of LiCu

The lowest frequency band observed with certainty using $308.06 \pm 0.13\,\text{nm}$ ($4.025 \pm 0.002\,\text{eV}$) radiation for photoionization occurs at $20\,478\,\text{cm}^{-1}$ ($2.539\,\text{eV}$) and is listed in Table I as the probable 0-0 band of the $[20.5]^1\Sigma^+ \leftarrow X^1\Sigma^+$ system. This places an upper limit on the ionization energy of the molecule as $6.566\,\text{eV}$. The highest energy band of the progression reported here, the 31-0 band at $24\,905\,\text{cm}^{-1}$ ($3.088\,\text{eV}$), is also the highest energy feature recorded using the dye fundamental in combination with $308\,\text{nm}$ radiation for photoionization. When the $308\,\text{nm}$ radiation was blocked the ion signal disappeared, indicating that two photons of the $24\,905\,\text{cm}^{-1}$ radiation were not sufficiently energetic to ionize the molecule. This places a lower limit on the ionization energy of $6.176\,\text{eV}$. We therefore report the ionization energy of LiCu as $\text{IE}(\text{LiCu}) = 6.37 \pm 0.20\,\text{eV}$, where the error limits are chosen to encompass the upper and lower limits.

The measured ionization energy of LiCu may be used to infer the bond energy of the LiCu^+ cation, which dissociates to Li^+ , $1s^2, ^1S + \text{Cu}$, $3d^{10}4s^1, ^2S$. From the thermochemical cycle

TABLE II. Fitted spectroscopic constants of LiCu.^a

Electronic state	Constant	⁷ Li ⁶³ Cu	⁷ Li ⁶⁵ Cu
[20.5] ¹ Σ ⁺	T_0	20 548.97(8.88)	20 547.64(8.67)
	ω'_e	152.34(2.74)	152.63(2.67)
	$\omega'_e x'_e$	1.318(252)	1.366(246)
	$\omega'_e y'_e$	0.051 1(95)	0.053 0(93)
	$\omega'_e z'_e$	-0.000 67(13)	-0.000 69(12)
	B'_e	0.366 34(79)	0.342 74(89)
	α'_e	0.016 5(17)	0.009 8(8)
	γ'_e	0.000 91(13)	0.000 29(4)
	δ'_e	-1.83(31) × 10 ⁻⁵	...
	r'_e	2.700 0(29) Å	2.787 1(36) Å
X ¹ Σ ⁺	B''_0	0.522 02(16)	0.519 73(21)
	r''_0	2.261 8(3) Å	2.263 3(5) Å

^aAll spectroscopic constants are reported in cm⁻¹ except where noted otherwise. These constants are only capable of describing the levels $v' = 6 - 31$ of the [20.5] ¹Σ⁺ state. Serious deviations are found when they are used to predict the energies of the $v' = 0 - 5$ levels. Other properties of LiCu determined in this work or that of Ref. 5 are $D_0(\text{LiCu}) = 1.9451 \pm 0.0015$ eV, $\text{IE}(\text{LiCu}) = 6.37 \pm 0.20$ eV, and $D_0(\text{Li}^+ - \text{Cu}) = 0.97 \pm 0.20$ eV.

$$D_0(\text{Li}^+ - \text{Cu}) = D_0(\text{LiCu}) + \text{IE}(\text{Li}) - \text{IE}(\text{LiCu}), \quad (3.5)$$

and the values of $D_0(\text{LiCu}) = 1.9451 \pm 0.0015$ eV,⁵ $\text{IE}(\text{LiCu}) = 6.37 \pm 0.20$ eV, and $\text{IE}(\text{Li}) = 5.392$ eV,⁷ a value of $D_0(\text{Li}^+ - \text{Cu}) = 0.97 \pm 0.20$ eV is obtained. The weaker bond energy of LiCu⁺ as compared to LiCu is a direct consequence of it possessing only a single electron in the σ bonding orbital, as opposed to the two electrons present in neutral LiCu.

IV. DISCUSSION

As expected, the ground state of LiCu has been shown to be X ¹Σ⁺, with a $3d_{\text{Cu}}^{10}\sigma^2$ molecular configuration correlating to the $\text{Li}(1s^2 2s^1, ^2S) + \text{Cu}(3d^{10} 4s^1, ^2S)$ atomic ground states. Its bond length is best estimated by averaging the values obtained for the ⁷Li⁶³Cu and ⁷Li⁶⁵Cu isotopic modifications, resulting in $r_0(X \text{ } ^1\Sigma^+) = 2.2625(8)$ Å. This information complements the value of the bond energy reported by Brock *et al.*, $D_0(\text{LiCu}) = 1.9451 \pm 0.0015$ eV,⁵ and the measured ionization energy, $\text{IE}(\text{LiCu}) = 6.37 \pm 0.20$ eV, obtained in the present investigation.

In contrast to the ground state, the [20.5] ¹Σ⁺ excited state has a rather long bond, with $r'_e = 2.74(4)$ Å obtained as an average of ⁷Li⁶³Cu and ⁷Li⁶⁵Cu. Likewise, this state is characterized by a greatly reduced vibrational frequency (152 cm⁻¹) as compared to either the measured value (465.9 cm⁻¹) (Ref. 5) or the theoretically calculated values [379 cm⁻¹ (Ref. 9) or 356 cm⁻¹ (Ref. 10)] for the ground state. These facts may be employed to suggest a separated atom asymptote to which the [20.5] ¹Σ⁺ state may correlate.

The lowest excited separated atom limit in the Li+Cu system corresponds to $\text{Li } 1s^2 2s^1, ^2S_0 + \text{Cu } 3d^9 4s^2, ^2D_{5/2}$ and lies 11 202.57 cm⁻¹ above ground state atoms.⁷ This separated atom limit will generate a ¹Σ⁺ state corresponding to a $3d_{\text{Cu}}^9(^2\Sigma^+) \sigma^2 \sigma^{*1}$ molecular configuration, which has a bond order of 0.5 and will have a bond energy greatly reduced from that of the ground state due to the occupation of the σ^* orbital. To estimate the bond energy expected for this

state we note that the LiCu⁺ cation possesses a ground configuration of $3d_{\text{Cu}}^{10}\sigma^1, X \text{ } ^2\Sigma^+$ and also has a bond order of 0.5. The estimated bond energy obtained above for the LiCu⁺ cation is $D_0(\text{Li}^+ - \text{Cu}) = 0.97 \pm 0.20$ eV, suggesting that a similar value might be expected for the $3d_{\text{Cu}}^9(^2\Sigma^+) \sigma^2 \sigma^{*1}, ^1\Sigma^+$ state of neutral LiCu.

Assuming for the moment that the [20.5] ¹Σ⁺ state of LiCu does correlate to the $\text{Li } 2s^1, ^2S_0 + \text{Cu } 3d^9 4s^2, ^2D_{5/2}$ separated atom limit at 11 202.57 cm⁻¹,⁷ using the bond energy reported by Brock *et al.*, $D_0(\text{LiCu}) = 1.9451 \pm 0.0015$ eV,⁵ and the frequency of the 0-0 band (ν_{00}) the bond energy of the [20.5] ¹Σ⁺ state may be deduced to be

$$D_0([20.5] \text{ } ^1\Sigma^+) = D_0(X \text{ } ^1\Sigma^+) + \text{AE} - \nu_{00}, \quad (4.1)$$

where AE gives the energy of the excited separated atom limit to which the [20.5] ¹Σ⁺ state correlates (11 202.57 cm⁻¹). This provides an estimated bond energy of the [20.5] ¹Σ⁺ state of 6413 cm⁻¹ (0.80 eV), a value in reasonable agreement with the expectation of 0.98 ± 0.22 eV based on the value of $D_0(\text{Li}^+ - \text{Cu})$. Moreover, the poor bonding expected from the $3d_{\text{Cu}}^9(^2\Sigma^+) \sigma^2 \sigma^{*1}$ molecular configuration also explains the low vibrational frequency and long bond length of this state. Accordingly, it is considered likely that the [20.5] ¹Σ⁺ state correlates adiabatically to the $\text{Li } 1s^2 2s^1, ^2S_0 + \text{Cu } 3d^9 4s^2, ^2D_{5/2}$ separated atom limit.

The values of $B'_e, \alpha'_e, \gamma'_e, \delta'_e, \omega'_e, \omega'_e x'_e, \omega'_e y'_e,$ and $\omega'_e z'_e$ summarized in Table II were used to perform a Rydberg-Klein-Rees (RKR) calculation of the [20.5] ¹Σ⁺ potential using the RKR1 program of LeRoy.¹⁸ The result of this calculation is displayed in Fig. 4. In the RKR1 program¹⁸ one can smooth the curve when the inner wall begins to show unphysical phenomena such as unexpected inflection points or turning out upon itself. This is done by extrapolating the inner turning points using a model based on the previous three calculated points, and calculating the position of the outer turning point relative to the inner turning

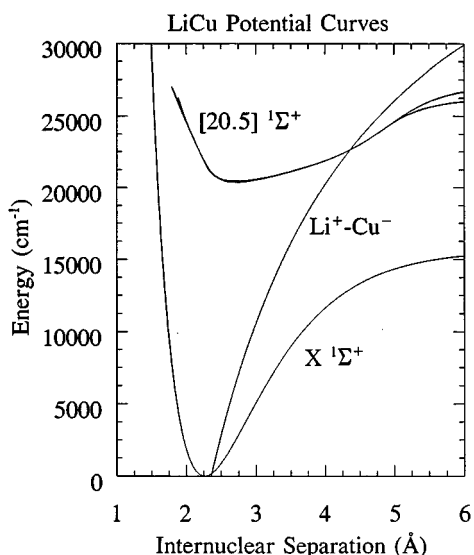


FIG. 4. Potential energy curves for the LiCu molecule. The ground state curve is drawn using a Morse potential based on the bond energy and vibrational frequency determination of Ref. 5. Four different RKR potential curves for the $[20.5] \ ^1\Sigma^+$ state are also presented as discussed in the text. Also shown is an electrostatic potential for the Li^+Cu^- ion-pair state, obtained by treating the ions as nonpolarizable point charges.

point. To draw Fig. 4 this smoothing procedure was required above $\nu' = 12$ ($22\ 255\ \text{cm}^{-1}$). In addition, to provide an estimate of the uncertainty in the RKR potential for the $[20.5] \ ^1\Sigma^+$ state this same procedure was followed to construct a RKR potential curve using the data for $^7\text{Li}^{65}\text{Cu}$ listed in Table II. Two additional RKR curves were constructed using vibrational parameters derived from a fit of the bands recorded in high resolution along with the $\nu' = 0-5$ levels listed in Table I. All four RKR curves are nearly coincident in the low energy region up to $25\ 000\ \text{cm}^{-1}$, providing confidence that the RKR potential in this energy range is qualitatively correct.

Also shown in Fig. 4 is the ground state potential energy curve based on a Morse potential using the bond energy [$D_0(\text{LiCu}) = 1.9451\ \text{eV}$] and vibrational frequency ($465.9\ \text{cm}^{-1}$) reported by Brock *et al.*⁵ In addition, a simple electrostatic potential for the $\text{Li}^+(1s^2, ^1S) + \text{Cu}^-(3d^{10}4s^2, ^1S)$ ion pair state, which must correspond to a state of $^1\Sigma^+$ symmetry, is plotted as $V(R) = D_0(\text{LiCu}) + \text{IE}(\text{Li}) - \text{EA}(\text{Cu}) - e^2/R$. This ion pair potential treats both Li^+ and Cu^- as nonpolarizable point charges and therefore both underestimates the attractive potential at large R and omits the repulsive potential at small R . These two effects tend to cancel on the outer limb of the curve, so that this estimated ion-pair potential can provide a useful guide for thinking about the electronic states and chemical bonding in the LiCu molecule.

It is immediately obvious from Fig. 4 that the RKR potential for the $[20.5] \ ^1\Sigma^+$ state displays an unusual shape. We believe this to be caused by avoided curve crossings between the $^1\Sigma^+$ states correlating diabatically to $\text{Li}(1s^2 2s^1, ^2S) + \text{Cu}(3d^{10} 4s^1, ^2S)$, $\text{Li}(1s^2 2s^1, ^2S)$

$+ \text{Cu}(3d^9 4s^2, ^2D)$, $\text{Li}^+(1s^2, ^1S) + \text{Cu}^-(3d^{10} 4s^2, ^1S)$, and possibly $\text{Li}(1s^2 2p^1, ^2P^o) + \text{Cu}(3d^{10} 4s^1, ^2S)$. The peculiar shape of the $[20.5] \ ^1\Sigma^+$ potential curve is reminiscent of the odd shape of the adiabatic potential curve of the $A \ ^1\Sigma^+$ state of LiH, which was first investigated by Mulliken in 1936 (Ref. 19) and has recently been studied by Boutalib and Gadéa.²⁰ These investigators have computed both diabatic and adiabatic potential curves for LiH and find that the $X \ ^1\Sigma^+$ ground state correlates diabatically to the $\text{Li}^+ + \text{H}^-$ ion pair state. The long range attraction between the separated Li^+ and H^- ions leads to multiple curve crossings as one moves to shorter distances on the $\text{Li}^+ + \text{H}^-$ potential in the diabatic representation, but these become avoided curve crossings in the adiabatic representation. The net result is some very odd-looking adiabatic potential curves for the $^1\Sigma^+$ states of LiH. The enhanced electron affinity of Cu ($1.228\ \text{eV}$) (Ref. 21) as compared to H ($0.754\ 209\ \text{eV}$) (Ref. 21) suggests that the ion pair state will be at least as important in LiCu as it is in LiH. Moreover, the fact that the extrapolated ion-pair curve (neglecting polarization of Cu^- and Pauli repulsion of the ion cores) comes close to the minimum of the $X \ ^1\Sigma^+$ ground state potential suggests very strongly that the LiCu ground state is primarily ionic in character, corresponding to $\text{Li}^+ + \text{Cu}^-$.

It has previously been noted that the bond lengths of Cu_2 , CuAg , CuAu , Ag_2 , and Au_2 may be reproduced to an accuracy of $0.012\ \text{Å}$ by assigning covalent bond radii of 1.107 , 1.263 , and $1.233\ \text{Å}$ to Cu, Ag, and Au, respectively.²² This is indicative of the similarity in the chemical bonding of these molecules. One might think that with the addition of Li_2 and LiCu to this set of molecules a covalent bond radius might be deduced for Li. Using the experimental bond lengths of Li_2 ($2.6729\ \text{Å}$) (Ref. 23) and LiCu ($2.263\ \text{Å}$, this work), however, it is found that the required covalent radius of Li is $1.336\ \text{Å}$ (for Li_2) and $1.156\ \text{Å}$ (for LiCu). The much smaller value of r_{Li} required to reproduce the bond length of LiCu as compared to Li_2 demonstrates that the chemical bonding is not at all similar in these two species. While Li_2 is dominated by covalent bonding, the ground state of LiCu is dominated by ionic bonding, and is best described as Li^+Cu^- . The small size of the Li^+ ion then leads to a much shorter bond than would be expected from the average of the covalent Li_2 and Cu_2 bond lengths. In this regard the short bond length of LiCu provides strong support for its assignment as an ionic molecule.

V. CONCLUSION

Resonant two-photon ionization spectroscopy has been used to study jet-cooled LiCu. Together with a forthcoming paper on LiCa this study will provide a means of understanding the different interactions between alkali metals and the $3d^{n+1}4s^1$ metals (like Cu) and $3d^n4s^2$ metals (like Ca). The present study of LiCu has identified the $[20.5] \ ^1\Sigma^+ \leftarrow X \ ^1\Sigma^+$ band system, and analysis of the spectrum has provided $r_0(X \ ^1\Sigma^+) = 2.2625(8)\ \text{Å}$, $r_e([20.5] \ ^1\Sigma^+) = 2.74(4)\ \text{Å}$, and $\omega'_e([20.5] \ ^1\Sigma^+) = 152.3(2.7)\ \text{cm}^{-1}$. The

short bond length of the $X^1\Sigma^+$ state indicates that this molecule is primarily ionic (Li^+Cu^-) in its ground state.

ACKNOWLEDGMENTS

Research support from the National Science Foundation under Grant Nos. CHE-9215193 and CHE-9626557 is gratefully acknowledged. The donors of the Petroleum Research Fund, administered by the American Chemical Society, are also acknowledged for partial support of this research.

¹See, for example, M. D. Morse, *Adv. Metal Semicond. Clusters* **1**, 83 (1993); J. C. Pinegar, J. D. Langenberg, C. A. Arrington, E. M. Spain, and M. D. Morse, *J. Chem. Phys.* **102**, 666 (1995).
²J. M. Behm and M. D. Morse, *Proc. SPIE-Int. Soc. Opt. Eng.* **2124**, 388 (1994); *J. Chem. Phys.* **101**, 6500 (1994).
³L. M. Russon, G. K. Rothschof, P. B. Armentrout, M. D. Morse, A. I. Boldyrev, and J. Simons, *J. Chem. Phys.* (to be submitted).
⁴H. P. Bonzel, *J. Vac. Sci. Technol. A* **2**, 866 (1984).
⁵L. R. Brock, A. M. Knight, J. E. Reddic, J. S. Pilgrim, and M. A. Duncan, *J. Chem. Phys.* **106**, 6268 (1997).
⁶A. Neubert and K. F. Zmbrov, *Trans. Faraday Soc.* **70**, 2219 (1974).
⁷C. E. Moore, *Atomic Energy Levels*, Natl. Bur. Stand. Circ. No. 467 (U.S. GPO, Washington, D.C., 1971).
⁸H.-O. Beckmann, G. Pacchioni, and G.-H. Jeung, *Chem. Phys. Lett.* **116**, 423 (1985).
⁹C. W. Bauschlicher, Jr., S. R. Langhoff, H. Partridge, and S. P. Walch, *J. Chem. Phys.* **86**, 5603 (1987).
¹⁰D. B. Lawson and J. F. Harrison, *J. Phys. Chem.* **100**, 6081 (1996).

¹¹L. M. Russon, S. A. Heidecke, M. K. Birke, J. Conceicao, P. B. Armentrout, and M. D. Morse, *Chem. Phys. Lett.* **204**, 235 (1993); L. M. Russon, S. A. Heidecke, M. K. Birke, J. Conceicao, M. D. Morse, and P. B. Armentrout, *J. Chem. Phys.* **100**, 4747 (1994).
¹²Similar in design to that described in S. C. O'Brien, Y. Liu, Q. Zhang, J. R. Heath, F. K. Tittel, R. F. Curl, and R. E. Smalley, *J. Chem. Phys.* **84**, 4074 (1986).
¹³W. C. Wiley and I. H. McLaren, *Rev. Sci. Instrum.* **26**, 1150 (1955).
¹⁴S. Gerstenkorn and P. Luc, *Atlas du Spectre d'Absorption de la Molécule d'Iode* (CNRS, Paris, 1978); S. Gerstenkorn and P. Luc, *Rev. Phys. Appl.* **14**, 791 (1979).
¹⁵D. J. Clouthier and J. Karolczak, *Rev. Sci. Instrum.* **61**, 1607 (1990).
¹⁶G. Herzberg, *Molecular Spectra and Molecular Structure I. Spectra of Diatomic Molecules* (Van Nostrand Reinhold, New York, 1950).
¹⁷See AIP Document No: PAPS JCPSA 6-107-1079-10 for 10 pages of absolute line positions. Order by PAPS number and journal reference from American Institute of Physics, Physics Auxiliary Publication Service, Carolyn Gehlbash, 500 Sunnyside Boulevard, Woodbury, NY 11797-2999. Fax: 516-576-2223, e-mail: paps@aip.org. The price is \$1.50 for each microfiche (48 pages) or \$5.00 for photocopies up to 30 pages, and \$0.15 for each additional page over 30 pages. Airmail additional. Make checks payable to the American Institute of Physics.
¹⁸R. J. LeRoy, *Chemical Physics Research Report*, CP-425 (University of Waterloo, Waterloo, 1992).
¹⁹R. S. Mulliken, *Phys. Rev.* **50**, 1017, 1028 (1936).
²⁰A. Boutalib and F. X. Gadéa, *J. Chem. Phys.* **97**, 1144 (1992).
²¹H. Hotop and W. C. Lineberger, *J. Phys. Chem. Ref. Data* **14**, 731 (1985).
²²M. D. Morse, *Adv. Metal Semicond. Clusters* **1**, 83 (1993).
²³K. P. Huber and G. Herzberg, *Molecular Spectra and Molecular Structure IV. Constants of Diatomic Molecules* (Van Nostrand Reinhold, New York, 1979).